Investigation of transient linear and circular birefringence in metallic thin films

R Wilks, N D Hughes and R J Hicken

School of Physics, University of Exeter, Stocker Road, Exeter EX4 4QL, UK

E-mail: r.j.hicken@exeter.ac.uk

Abstract
Optical pump–probe measurements have been performed on three materials
with pump pulses of 120 fs duration and variable helicity. The samples were
probed in a reflection geometry. We compare the transient intensity and rotation
signals induced in intrinsic GaAs wafers and sputtered polycrystalline Ni and
Al thin films. An initial peak is observed in the transient rotation signal. The
dependence of the peak height on the polarization of the pump is found to be
qualitatively different for the three materials, indicating different amounts of
linear and circular birefringence in each case. For ferromagnetic Ni the peak
is superimposed on a longer-lived ultra-fast demagnetization signal. For GaAs
and Al we also observe a tail in the rotation signal that decays on time-scales of
several picoseconds. In the case of GaAs, we attribute this to the relaxation of a
spin polarization that is induced by the pump beam within the thermal electron
population. In the case of Al, the dependence of the amplitude of the tail on the
pump beam's polarization is characteristic of linear birefringence. We suggest
that this signal is associated with an ultra-fast excitation of the lattice rather
than with optical orientation of spin.

1. Introduction

In recent years the development of ultra-fast optical pump–probe techniques has allowed
transient phenomena in solids to be studied with sub-picosecond temporal resolution. Heat
transfer between electrons and the lattice, propagation of thermo-elastic waves, and the
relaxation of the electron spin may clearly be observed [1]. Measurements of spin relaxation
are particularly relevant to the burgeoning field of spin electronics. For example, reduced spin
relaxation times lead to reduced giant magneto-resistance (GMR) in spin-valve structures,
while fast spin relaxation is of interest in magneto-optical recording technology as part of the
write process, and in the construction of fast magneto-optical modulators.

Pumping with linearly (circularly) polarized light may be used to transfer linear (angular) momentum to the electrons in a solid and induce a transient linear (circular) birefringence that causes the polarization state of a time-delayed probe beam to be modified. To lowest order, the pump–probe process may be regarded as a cubic non-linearity, involving two pump photons and one probe photon, that is predicted to exist from symmetry arguments [2]. Due to the rapid scattering of the electron momentum in real space, the induced birefringence might be expected to relax within tens of femtoseconds. However, in certain semiconductors, due to the spin–orbit splitting of the valence band, a circularly polarized pump can selectively excite spin-polarized electrons. For example, spin-polarized electrons have been excited from GaAs to the vacuum level and used in inverse photoemission experiments [3]. By pumping close to the band gap, non-equilibrium spin polarizations may be created that persist for times in excess of 1 ns and hence give rise to long-lived circular birefringence [4].

Spin relaxation effects in semiconductors and quantum well structures have been studied intensively [5]. The coherent control of spin orientation has been demonstrated in experiments performed at low temperatures and in high magnetic fields, and using the optical Stark effect [6]. Recently, spin relaxation has also been studied at room temperature in the absence of external fields in experiments performed with ultra-short laser pulses [7]. This work has revealed a more complicated magneto-optical response on sub-picosecond timescales. Three separate processes were identified and the physical origin of two of these was inferred by studying their dependence on the wavelength of the pump beam. The process with the longest relaxation time is associated with the spin polarization of the thermalized electron distribution. A faster signal results from the bleaching of the spin-selective optical transition prior to thermalization. Finally a strong peak, centred at zero time delay, is observed within the overlap of the pump and probe pulses. This is associated with the orbital and spin angular momentum of the optically excited hot electrons.

The peak at zero delay has been observed in semiconductors [8] and both non-magnetic [9] and ferromagnetic [10] metals. The observation of the peak in Ni led to suggestions that the effect might be used in an optical auto-correlator [11]. In ferromagnetic materials an additional transient rotation signal may be observed due to the ultra-fast demagnetization effect, in which the spontaneous magnetization is reduced following excitation with an intense femtosecond laser pulse. The first measurements of a partial demagnetization in Ni showed that the demagnetization takes place within a time delay of 260 fs [12] or 280 fs [13]. A complete demagnetization to the paramagnetic state was observed for $CoPt_3$ [14] and in ultra-thin Ni films [15] where the Curie temperature is reduced relative to that of the bulk metal. Theory suggests that the demagnetization results from the combined action of the spin–orbit coupling and the external laser field [16] and that the intrinsic decay time may be as short as 10 fs [17]. Measurements made with a magnetic second harmonic generation (SHG) probe provide some support for this claim [18]. However, doubts have arisen about whether magneto-optical measurements made at time delays of less than 2 ps truly reflect the magnetic state of the sample. It has been suggested that non-magnetic effects can contribute to the measured signal that is obtained with both linear [19, 20] and non-linear [21, 22] magneto-optical probes. The most recent measurements made on $CoPt_3$ with 20 fs pulses show that the magneto-optical signal does indeed represent the magnetic state after 50 fs, which is the electron thermalization time for this material [23]. Our own recent work with a linearly polarized pump beam [24] has shown that it is important to study the ultra-fast demagnetization effect in the presence of a large saturating magnetic field or else much slower domain reorientation processes may contribute to the observed signal. So far, only a few studies of ultra-fast demagnetization have been performed with a circularly polarized pump [25] and, to our knowledge, no such studies have been made of nickel.

The pumping of non-magnetic metals with circularly polarized light is potentially of great interest, since the optical orientation of a non-equilibrium spin population would allow the spin relaxation time of conduction electrons to be determined from the transient rotation signal. For cubic metals at room temperature, where dephasing is insignificant due to motional narrowing, the transverse spin relaxation time, T_2, is expected to be equal to the longitudinal spin relaxation time, T_1. The theory of spin relaxation in metals is well established [26, 27] and involves the influence of spin–orbit coupling during momentum scattering. However, detailed quantitative calculations have only recently become available and these highlight the importance of spin 'hot-spots' on the Fermi surface [28] in reducing the value of T_1 for certain metals.

In the case of Al, the value of T_1 was calculated to be of the order of 100 ps at room temperature [29], in good agreement with room-temperature conduction electron spin resonance (CESR) data [30], and should be measurable in a femtosecond pump–probe experiment. Al is an excellent candidate for optical orientation experiments by virtue of its band structure. A direct interband transition between parallel bands on the square face of the Brillouin zone [31] leads to a strong optical absorption at a wavelength of about 800 nm that is well matched to the peak output of a mode-locked Ti:sapphire laser. In previous measurements made on metals such as Au [9], only intraband transitions were excited, so no comparison could be made with the interband pumping mechanism that is used to optically orient spins in GaAs. However, a further consequence of the interband transition in Al is a strong piezo-optic response at a wavelength of 800 nm [32]. Recently it was shown that both thermal and elastic transients must be considered in order to understand the rise of the transient reflectivity signal in Al [33]. In addition, a rapid surface melting was observed in measurements made with very large pump fluences, and attributed to an ultra-fast collapse of the band structure [34]. Therefore, we anticipate that an ultra-fast excitation of the lattice may also occur in pump–probe experiments.

In this paper we compare the change in intensity and rotation of the probe beam that is reflected from GaAs, Ni and Al samples following excitation with 120 fs laser pulses of different helicity. In general, transmission measurements [23] or measurements at different angles of incidence [34] are required to fully characterize the time evolution of all the relevant optical constants and elucidate the microscopic origin of the optical response. However, our aim here is only to investigate the characteristic time-scales. We show that, in each case, the transient rotation signal contains at least two components with different time dependence. We investigate the dependence of these different contributions on the pump fluence in GaAs, while we study the co-existence of the zero-delay peak and the ultra-fast demagnetization signal in Ni. We present measurements of a long-lived optical rotation signal in Al and discuss whether the signal is the result of the optical orientation of spin or is of piezo-optical origin. Finally, we compare the dependence of the zero-delay peak on the pump helicity within the three materials and determine the relative amounts of linear and circular birefringence present in each case.

2. Experiment

Measurements were made on intrinsic GaAs(100) wafers (Hall mobility 7000–8000 cm^2 V^{-1} s^{-1}, carrier density 1.5–6.5 $\times$ 10^7 cm^{-3}) and on 500 Å thick polycrystalline Ni and Al films grown on Si(100) wafers by dc magnetron sputtering. The Si substrates were chosen for their high thermal conductivity and optical flatness. The film thicknesses were chosen to be greater than the optical skin depth, yet sufficiently small so as to avoid roughening of the film surface that could lead to diffuse scatter in the optical measurements. We will see that pump-induced changes in the reflectivity of the films are sufficiently small
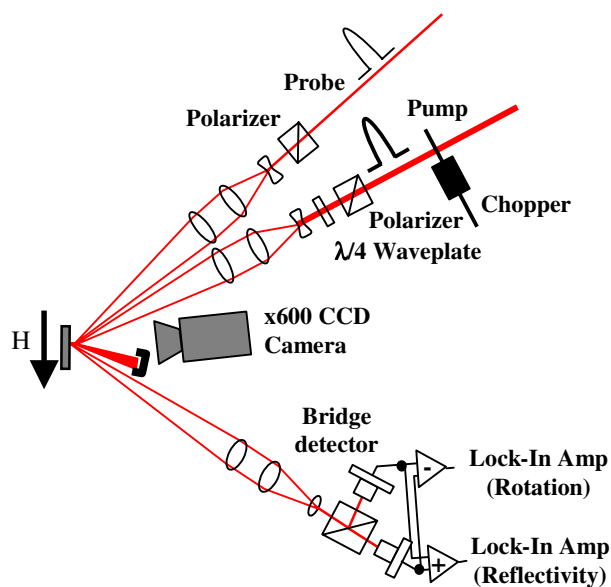
Figure 1. The geometry of the experiment.

(This figure is in colour only in the electronic version)

that the effect of the substrate on the optical response may be neglected throughout the present study. No overlayer was deposited, since thin self-passivating oxide layers are expected to form on these materials.

Optical pump–probe measurements were made with a Ti:sapphire laser that produced pulses of 800 nm in wavelength at a 82 MHz repetition rate. The beam was split into pump and probe parts, with average powers of 280 and 12 mW, respectively. The pump and probe beams were incident on the sample at angles of 25° and 47°, respectively, and the probe beam was p-polarized. The relatively large angle of incidence used for the probe beam means that the probe is sensitive to both in-plane and out-of-plane components of the magnetization through the longitudinal and polar magneto-optical Kerr effect (MOKE), respectively. The polarization of the pump beam could be varied continuously from a p-polarized state to a circularly polarized state by rotating a quarter wave plate placed after the polarizer. Both pump and probe beams were expanded by a factor of ten in order to reduce the beam divergence and focused to a 15 μm spot diameter, yielding a maximum pump fluence of about 2 mJ cm^{-2}. The pump and probe spots were carefully overlapped by moving the final focusing lenses on precision three-axis translation stages, while being viewed with a CCD camera that gave a $\times$600 on-screen magnification factor. The initial alignment and overlap of the focused spots was carried out on a clean, polished GaAs test sample so that the luminescence from the focused spots could be imaged with minimal diffuse scatter.

The temporal widths of the pump and probe pulses were checked with a fringe-resolved auto-correlator, placed just before the expansion optics, and found to be about 120 fs. The experimental geometry is shown in figure 1. A variable optical delay line in the pump beam path allowed the delay between pump and probe to be varied by up to 2 ns, with a minimum step size of 1.67 fs. The position of the retro-reflector in the delay line was varied through a few wavelengths at high frequency to remove coherence oscillations around the zero-delay position that result largely from interference of the probe beam with diffusely scattered pump

light. The reflected probe beam was directed into an optical bridge detector that allowed the reflectivity (sum signal) and rotation (difference signal) to be measured simultaneously.

Some care must be taken in setting the plane of polarization of the incident probe beam. We wish to detect the time-dependent rotation of an initially linearly polarized probe beam that arises from pump-induced changes in r_{sp} or r_{ps}. These reflection coefficients may be modified through changes in either the magnetization or the optical constants of the sample [35]. In our experiments the fractional change in the magnetization after the electron system has thermalized is expected to be much larger than the fractional change in the optical constants, so magnetic changes should dominate the changes in r_{sp} and r_{ps}. However, pump-induced changes in r_{ss} and r_{pp} will also cause rotation and ellipticity to appear on a probe beam that is not initially s or p polarized. We begin by setting the plane of polarization of the probe beam parallel to that of the optical table. The plane of incidence is generally rotated slightly relative to the plane of the table because the sample is never exactly vertical, and because the focusing lenses must be moved in order to overlap the pump and probe spots. When a non-magnetic sample is pumped with linearly polarized light, there are generally two contributions to the pump-induced rotation or ellipticity. Firstly, if the plane of polarization of pump and probe are different, a peak at zero time delay is observed due to the specular optical Kerr effect (SOKE). Secondly, if the probe is not precisely s or p polarized, there will be a breakthrough of the reflectivity signal that persists for hundreds of picoseconds. We suppress the SOKE peak by setting the pump polarization close to p, and then set the probe beam polarization to remove the reflectivity breakthrough so that the difference signal from the bridge is independent of the delay time. For a magnetic sample, a strong rotation signal is expected when the pump beam is linearly polarized due to the ultra-fast demagnetization effect. It is then more difficult to set the probe beam polarization correctly. However, the ultra-fast demagnetization signal may be identified if pairs of measurements are made with magnetic fields of opposite sign. Only the demagnetization signal is expected to change sign as the field is reversed, so it may be obtained unambiguously by taking half the difference of the signals obtained for positive and negative applied field [24].

3. Results

3.1. Gallium arsenide

Measurements were first made on the GaAs wafer with different pump beam polarizations. The time-dependent Kerr rotation, $\Delta\theta(t)$, obtained for linearly and circularly polarized pump beams, is shown in figure 2. The peak that was observed with a circularly polarized pump is approximately 100 mdeg high for a pump power of 200 mW, while the peak in the inset reflectivity signal is typically a few tenths of a per cent in height. In fact, three components can be distinguished in the rotation response that was obtained with a circularly polarized pump. First, there is a sharp peak, centred on zero delay, with a full width half maximum (FWHM) of 160 fs. Second, there is a contribution that is visible on the right-hand flank of the peak where the signal changes sign and which decays exponentially with a short time constant. Third, there is a contribution that decays exponentially but with a longer time constant. Let us assume that the laser pulse has a Gaussian profile, given by

$$I(t) \propto \frac{1}{\sqrt{2\pi}w} \exp\left(-\frac{t^2}{2w^2}\right). \tag{1}$$

The FWHM of the laser pulse is given by $2\sqrt{2\ln 2}\,w$, corresponding to a FWHM of $4\sqrt{\ln 2}\,w$ for the auto-correlation signal. The form of the expected magneto-optical response may be
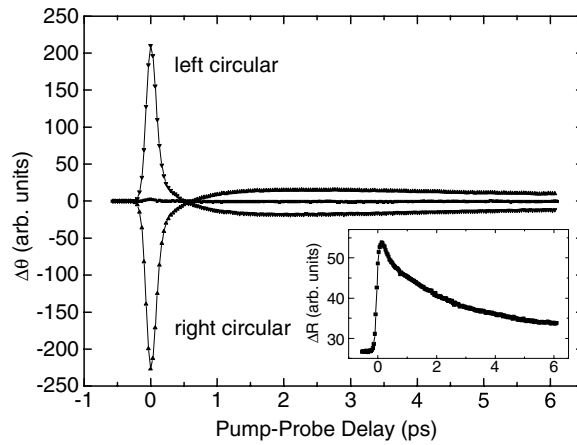
Figure 2. The time-dependent Kerr rotation, $\Delta\theta$, obtained from GaAs for the case of a linear, right and left circularly polarized beam. The pump power was 200 mW. The inset shows the time-resolved reflectivity signal.

obtained by convolving the functional form of each expected component (a δ function and two exponentials) with the pump and probe pulse profiles. This yields the following expression [7]:

$$\Delta\theta = A \exp\left(-\frac{t^2}{4w^2}\right) + \frac{B}{2} \exp\left(\frac{w^2}{\tau_1^2} - \frac{t}{\tau_1}\right)\left(1 - \mathrm{erf}\left(\frac{w}{\tau_1} - \frac{t}{2w}\right)\right)$$
$$+ \frac{C}{2} \exp\left(\frac{w^2}{\tau_2^2} - \frac{t}{\tau_2}\right)\left(1 - \mathrm{erf}\left(\frac{w}{\tau_2} - \frac{t}{2w}\right)\right), \tag{2}$$

in which A, B and C are the amplitudes of the three components, τ_1 and τ_2 are the decay constants of the exponential terms, and t is the time delay between the centres of the pump and probe pulses. Scans were recorded for four different cw-equivalent pump powers in the range of 10–200 mW, and the variation of the fitted parameter values is shown in figure 3. The Kerr rotation was also measured for intermediate elliptical pump polarization states by rotating the quarter wave plate in the pump beam. The dependence of the height of the peak at zero delay on ϕ is shown in figure 4, where ϕ is the angle that the fast axis of the quarter wave plate describes with the plane of polarization of the incident light. For settings of $0°$, $90°$, $180°$ and $270°$ the pump is linearly p-polarized and no magneto-optical signal is observed. At $45°$, $135°$, $225°$ and $315°$ the light is circularly polarized and the peak has maximum amplitude.

3.2. Nickel

Previously we reported measurements made on a thin-film Ni sample with a linearly polarized pump beam [24]. An ultra-fast demagnetization of approximately 7% was observed to occur within a time delay of less than 300 fs, in agreement with previous reports [12, 13]. In figure 5 we show the time dependences of the pump-induced reflectivity and Kerr rotation that were obtained with both linearly and circularly polarized pump beams. The shape of the reflectivity curve is not affected by the pump beam polarization. However, when the pump is circularly polarized a peak is observed at zero delay in addition to the ultra-fast demagnetization signal. The peak width is about 160 fs and is similar to that observed in GaAs. Measurements were made with a linear pump in the presence of large positive and negative magnetic fields. These fields were sufficient to saturate the sample, as can be seen from the inset hysteresis loop.
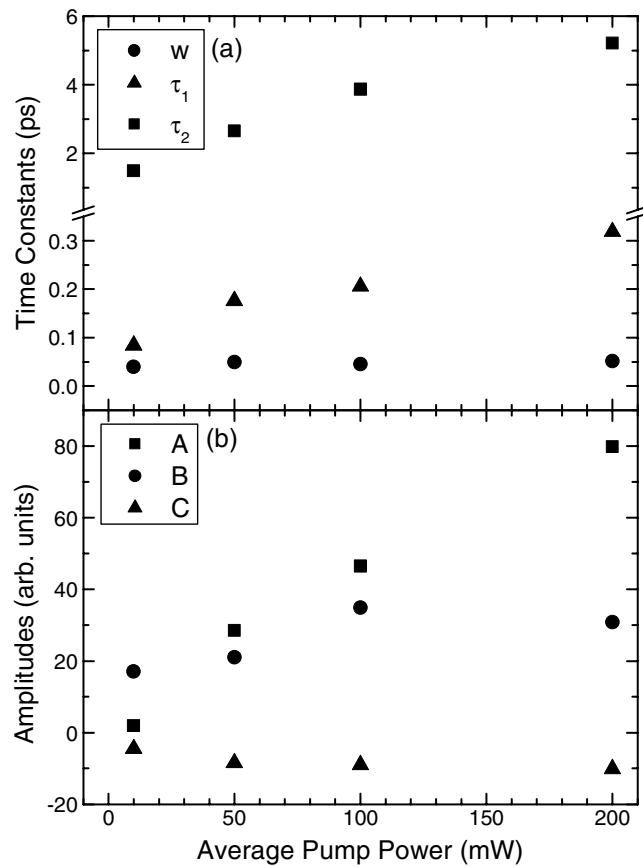
Figure 3. The dependence of the fitted parameters from equation (2) on the pump power for the GaAs sample.

Note that, although the pump-induced rotation has opposite sign for the two field directions, in each case it corresponds to a reduction in the magnitude of the spontaneous magnetization. There is an asymmetry in the two traces, so we obtain the true ultra-fast demagnetization signal by taking the average difference. The peak demagnetization signal is obtained at a time delay of approximately 200 fs.

We wish to comment on the fact that the two curves in positive and negative field appear to rise at slightly different times. We believe that this is due to a small residual zero-delay peak that does not change sign as the magnetic field is reversed. Indeed, the sum of the two curves shows a zero-delay peak of width identical to that of the zero-delay peak that is obtained with a circular pump. Although the pump beam is linearly polarized after the quarter wave plate, birefringence in the focusing optics may cause it to have a small ellipticity at the sample. It is therefore essential that there is no experimental uncertainty in the zero time-delay position if the curves obtained with a linear pump are to be compared correctly. The translation stage in our optical delay line does not possess encoders, so errors could in principle occur in the time delay. We therefore record the reflectivity signal simultaneously with all Kerr rotation scans, so that the reflectivity scans can then be overlaid to confirm the integrity of the zero-delay position in scans where no zero delay peak is observed.
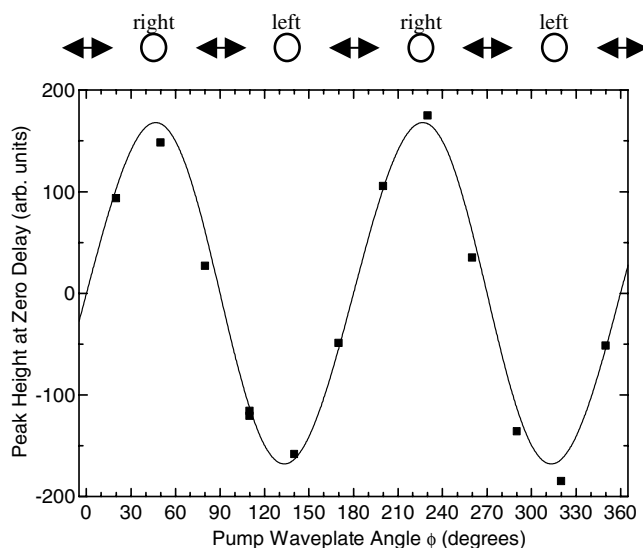
Figure 4. The dependence of the zero-delay peak height on the orientation of the quarter wave plate. The pump power was equal to 200 mW. The curve is a fit of equation (3) for which $A/B = -0.030$. The polarization state of the pump is sketched at the top of the panel.

The rise and decay times of the zero-delay peak are much faster than the rise time of the demagnetization signal. The zero-delay peak does not seem to be affected by the orientation of the magnetization of the sample, but is observed in addition to the normal demagnetization signal. Again, the height of the zero-delay peak depends on the pump polarization and has opposite sign for pump beams of opposite helicity. However, the dependence of the peak height on the degree of circular polarization is somewhat different to that in GaAs, as shown in figure 6.

3.3. Aluminium

Finally, the Al sample was examined. Since Al is non-magnetic, a p-polarized pump results in a flat rotation signal, as observed in GaAs. However, a rotation signal may generally be observed when the sample is pumped with elliptically polarized light, as shown in figure 7. The pump-induced change in reflectivity is also shown. The rotation signal contains both a peak at zero delay, again with a FWHM of 160 fs, and a longer-lived signal. We take the average difference of the curves in figure 7(b) as the best representation of the rotation signal obtained from the sample, as shown in figure 7(d). Equation (1) was then used to fit the data in figure 7(d). It was found that only one exponential term, analogous to the third term used in fitting the GaAs data, was required. In contrast to GaAs, we see that the rotation signal does not change sign. The time constant for the exponential decay was found to have a value of 6 ps. The dependence of the height of the zero-delay peak and the amplitude of the longer-lived contribution to the rotation signal on the orientation of the wave plate are shown in figure 8. The trend is completely different to that observed for GaAs (see figure 4). The rotation signal is seen to vanish when the pump is circularly polarized, whereas a maximum was observed for GaAs. The data in figure 8 has a period of only 90° and the signal has a maximum amplitude for a wave plate orientation of $\phi = \pm 22.5°$, at which the pump beam has elliptical polarization, as sketched above the figure. The amplitude of the exponentially decaying component was found to have a similar angular dependence to that of the zero-delay peak.
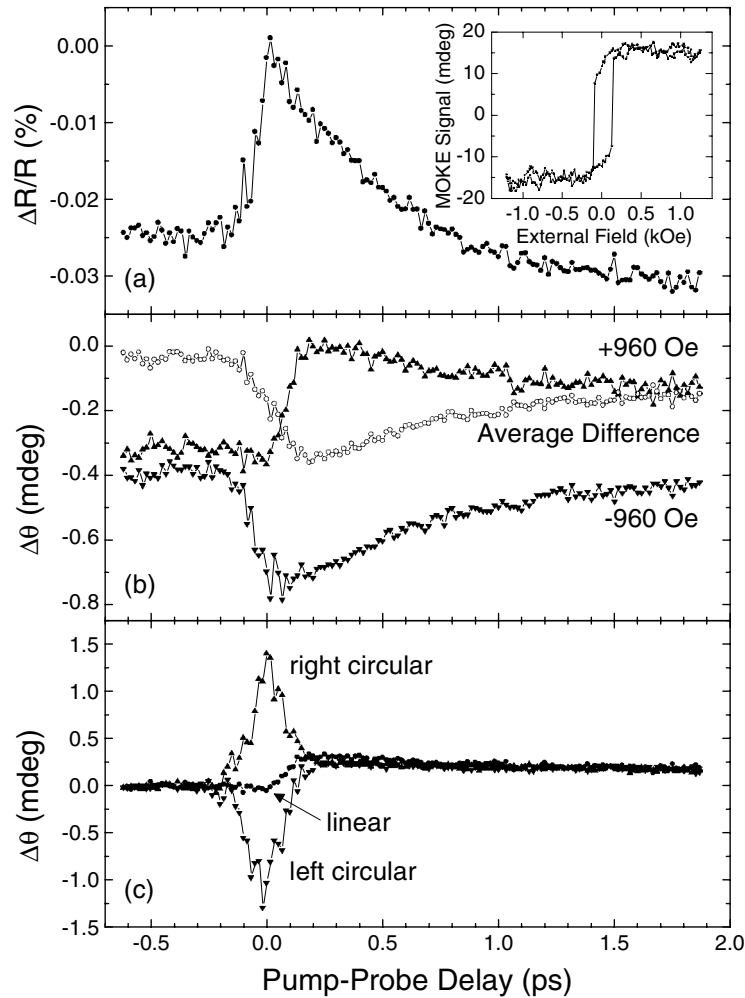
Figure 5. (a) The change in the reflectivity, ΔR, of the Ni sample induced by the pump beam. A quasi-static Kerr rotation hysteresis loop is shown in the inset. (b) The time-dependent Kerr rotation, $\Delta\theta$, obtained with a linearly polarised pump beam and positive and negative static magnetic fields. The ultra-fast demagnetization signal is obtained from the average difference signal, which is also shown. (c) The time-dependent Kerr rotation, obtained with linear and left and right circularly polarized pump beams. A magnetic field of +960 Oe was applied in each case, and a time-independent background signal has been subtracted from each trace.

4. Discussion

The measurements made on the GaAs sample demonstrate that high-quality data can be obtained with our measurement technique, as evidenced by figure 2, and used to establish a basis for comparison with measurements made on metals. Our results are qualitatively similar to those reported by Kimel *et al* [7], in that three separate contributions to the rotation signal have clearly been identified. Our measurements are made at a wavelength that is in the centre of the range used in [7], which corresponds to an energy of 1.55 eV that is well above the 1.42 eV room-temperature band gap of intrinsic GaAs. However, our pump fluence is one
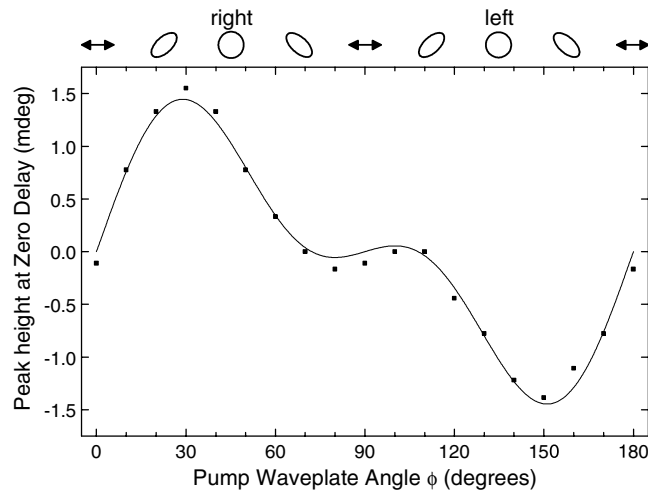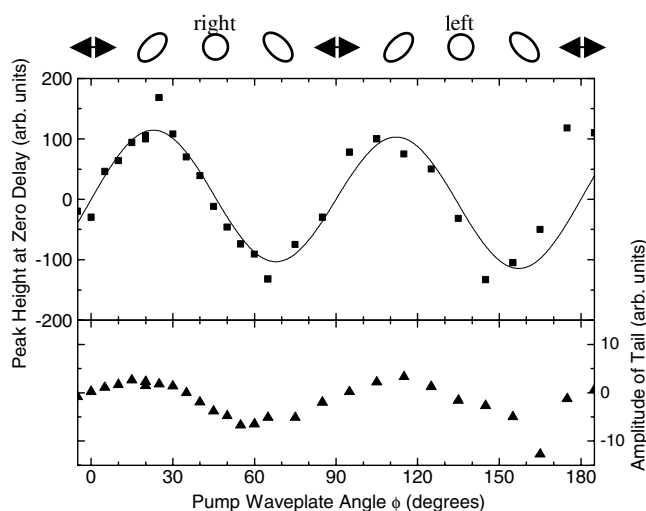
Figure 6. The dependence of the zero-delay peak height on the orientation of the quarter wave plate is shown for the Ni sample. The curve is a fit of equation (3) for which $A/B = 0.615$. The polarization state of the pump is sketched at the top of the panel.

to two orders of magnitude greater. The three amplitudes, A, B and C, are seen to exhibit a monotonic non-linear dependence on pump power. This suggests that interactions between excited carriers and renormalization of the band structure play an important role. While the width of the Gaussian peak at zero delay appears to be constant, the time constants for the two exponential terms both increase with pump power. Our values of τ_1 are longer than that of 30 fs reported in [7], while our value of τ_2 never reaches that of 10 ps reported by the same authors. The reason for these differences is currently unclear, although we conjecture that the detailed form of the rotation response may be highly sample dependent. Since the exponential term with the short time constant has been attributed to population effects, one might expect to see a component with similar time constant in the reflectivity data. However, no such component could be found when a form similar to equation (2) was fitted to the reflectivity data shown in the inset of figure 2.

The ultra-fast demagnetization that was observed in Ni when the pump is linearly polarized is in good agreement with previous reports by ourselves and others [12, 13, 24]. A peak is seen at zero delay, in addition to the ultra-fast demagnetization signal when the pump is circularly polarized. The demagnetization signal may, in principle, be removed by rotating the orientation of the static magnetic field through 90° to the transverse MOKE configuration [35]. We could not detect any effect of the pump helicity on the demagnetization signal on longer time-scales. This is not surprising if an interband transition is required for optical orientation of the thermalized electron population. We also note that the magneto-optical response of Ni should be more complicated than that of GaAs, because there are two different quantization axes to be considered. Firstly, the spontaneous magnetization lies in the plane of the sample and is sensed by means of the longitudinal MOKE. Secondly, since the pump beam is incident at an angle of 25°, any optically oriented spins should be aligned close to the sample normal and sensed by polar MOKE. However, the optically oriented spins would be expected to precess in the exchange field that is associated with the spontaneously magnetized electron population and rapidly dephase. Therefore, the effect of the pump helicity on the ultra-fast demagnetization is probably best studied in samples that are magnetized perpendicular to the plane and pumped
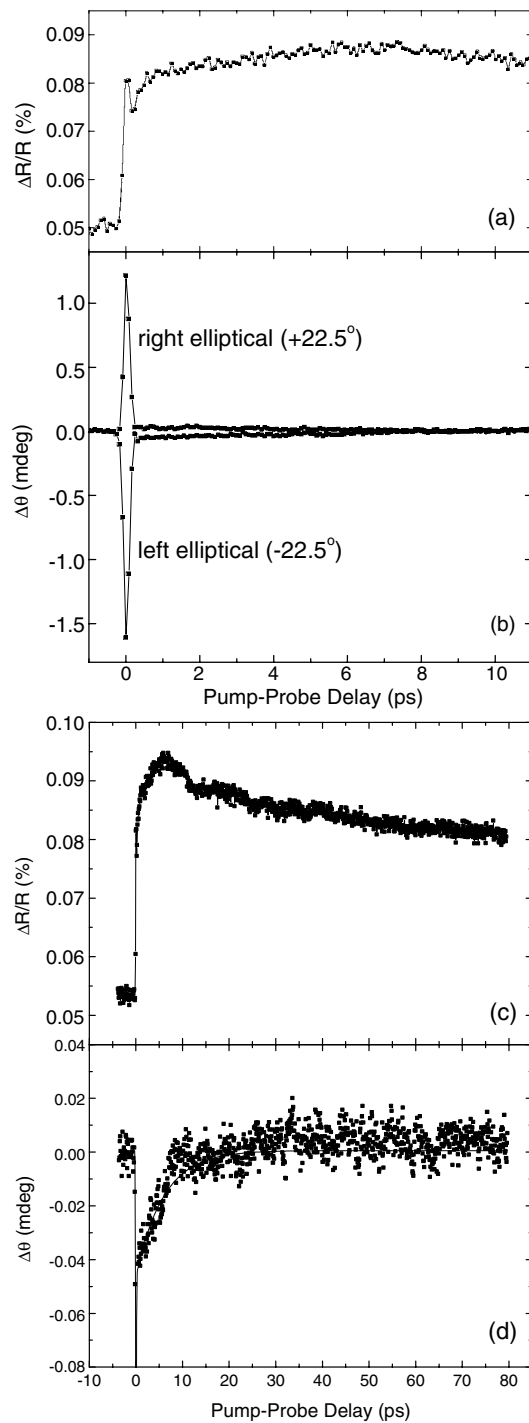
Figure 7. (a) The time dependence of the pump-induced change in reflectivity, ΔR, is shown for the Al sample. (b) The pump-induced Kerr rotation, $\Delta\theta$, from the Al sample. The orientation of the quarter wave plate was set to $\pm 22°$ so that the pump beam was elliptically polarized. (c) The reflectivity data is plotted on an extended time-scale. (d) The average difference of the data in panel (b) is plotted. The solid curve was obtained by fitting equation (2) to the data.

Figure 8. The dependence of the zero-delay peak height and the amplitude of the long-lived difference signal (shown in figure 7(d)) on the orientation of the quarter wave plate for the Al sample. The curve is a fit of equation (3) for which $A/B = 13.6$. The polarization state of the pump is sketched at the top of the panel.

at normal incidence. We note that a large magnetic field is required to overcome the shape anisotropy of the thin film, and that it is difficult to generate such a field with an electromagnet while maintaining wide field optical accesss.

The reflectivity signal that was observed in the Al film rises on a time-scale much longer than that observed for Ni and GaAs. A time-resolved photoemission study [36] showed that single electron states in Al have lifetimes of less than 200 fs at energies of greater than 0.5 eV above the Fermi level. It seems unlikely then that the reflectivity signal results purely from heating of the electron system, since the electron system thermalizes on sub-picosecond time-scales. Similarly long rise times were observed recently and explained by Richardson and Spicer [33]. In their model the optical pump initially heats the electron system, and heat is transferred to the lattice through electron–phonon scattering, so that the electron and phonon systems reach equilibrium within about 0.6 ps [37]. However, heating of the electron system creates a thermal stress that causes an acoustic pulse to propagate from the surface into the interior of the film. The rise time of the reflectivity signal is related to the time taken for the acoustic pulse to move out of the region (about one skin depth) sensed by the probe beam. Echoes are expected as the acoustic pulse is reflected from the film–substrate interface back into the optically probed region. We believe that this is the origin of the small dip in the data of figure 7(c) between 10 and 20 ps. A similar feature was observed for a 50 nm film that was studied in [34].

The dependence of the Al rotation signal on the pump helicity is one of the most surprising aspects of the present study. Since the pump beam is incident on the sample at an angle of 25°, one might expect the polarization of the electric field within the surface of the sample to be somewhat different to that outside the sample. However, this seems unlikely, since we have calculated the Fresnel transmission coefficients t_s and t_p and find that t_s is approximately equal to t_p in each case. Since peaks at zero delay were observed in all three samples, we may compare their behaviour. In each case, the FWHM of 160 fs corresponds to the expected width of the cross-correlation of two laser pulses of 120 fs pulse width. This suggests that the linear

or angular momentum imparted to the majority of the optically excited hot electrons relaxes on time-scales that are much shorter than the pulse width. The dependence of the peak height on pump helicity is completely different for GaAs and Al, while exhibiting an intermediate behaviour for Ni. A simple sinusoidal variation with a period of 180° was observed for GaAs in figure 4. It is easily shown that the difference in the number of photons of left and right circular polarization present in the pump beam is proportional to $\sin 2\phi$, so the angular dependence that was observed for GaAs is charactersitic of pump-induced circular birefringence. A general expression has been given in [2] for the rotation of the probe beam due to cubic non-linearity in an isotropic medium, for the case that both pump and probe beams are at normal incidence. The normal incidence formulae provide a reasonable approximation to the present situation, since the pump and probe beams within the sample are strongly refracted towards the film normal. In our experimental configuration, the incoherent contribution to the rotation induced on the probe beam is given by the following expression.

$$\theta = \frac{-32\pi^2 I_p}{c|1+n|^2}\left(\frac{A}{2}\sin 4\phi + B\sin 2\phi\right) \tag{3}$$

where

$$A = \mathrm{Re}\left(\frac{\chi_{xxyy} + \chi_{xyyx}}{n(1-n^2)}\right), \tag{4}$$

$$B = -\mathrm{Im}\left(\frac{\chi_{xxyy} - \chi_{xyyx}}{n(1-n^2)}\right), \tag{5}$$

n is the refractive index, I_p is the intensity of the pump beam, c is the speed of light in vacuum, and χ_{xxyy} and χ_{xyyx} are the non-vanishing components of the third-order susceptibility tensor. The first and second terms in equation (3) are associated with the optically induced linear and circular birefringence and are known as the SOKE and the specular inverse Faraday effect (SIFE), respectively. Our rotation measurements do not fully characterize the cubic susceptibility tensor, only the combination of components given in equations (4) and (5). From figures 4, 6 and 8 we might conclude that the SIFE dominates the zero-delay peak in GaAs [7], the SOKE is dominant in Al, while the more complicated dependence in Ni is the result of competition between the SIFE and the SOKE. No comprehensive microscopic theory of the cubic non-linearity has yet been advanced, and there is no reason to expect that similar behaviour should be observed in GaAs, Ni and Al, given their very different electronic structures.

From figure 8 we see that the slowly decaying tail and the zero-delay peak obtained in the Al rotation signal both exhibit a dependence on the pump polarization that is characteristic of linear birefringence. A purely electronic mechanism would require a either re-distribution of electronic charge that would be screened on femtosecond time-scales or a re-distribution of electronic momentum states that would be destroyed by momentum scattering on similarly short time-scales. An alternative mechanism is therefore required to explain the presence of the tail. One possibility is that the apparent rotation (difference) signal results from misalignment of the probe beam polarization. However, we were careful to use the alignment procedure described in section 2. We would also expect a signal resulting from changes in the optical constants of the sample to appear with the same sign in both the curves shown in figure 7(b). A second possibility is that the thermal electrons become spin-polarized, but this seems unlikely for two reasons. Firstly, the observed relaxation time of 6 ps is an order of magnitude smaller than the T_1 values obtained by calculation [29] and from CESR data [30]. Secondly, the dependence on the pump polarization beam would require a completely different mechanism for optical orientation to that which is well established in GaAs.

Finally, we consider whether the long-lived birefringence could result from a distortion of the lattice. The coherent phonon in [32] was generated by an isotropic thermal stress that would not be expected to produce birefringence. By fitting equation (2) to the reflectivity data in figures 7(a) and (c) we find that the rise of the reflectivity between 0.2 and 6 ps has a time constant of 2 ps, which is somewhat shorter than the value of 6 ps that was obtained from the rotation data. Therefore, if the slow rise of the reflectivity curve is due to propagation of the thermo-elastic wave, an additional mechanism is still required to explain the rotation data. From figure 7, the tail within the rotation signal appears to rise instantaneously, so it would be necessary for either the optical field to act directly on the ion cores within the lattice or for the lattice to respond to the short-lived redistribution of conduction electron momentum states induced by the optical field. The recent observation of ultra-fast surface melting in Al lends some support to this idea [34]. Indeed, it seems reasonable to expect that excitation of the bonding–anti-bonding transition in Al would be sensitive to the relative alignment of the optical electric field with a particular bond. We suggest then that a lattice excitation provides the most likely mechanism for the long-lived linear birefringence. Further insight into the origin of the effect might be gained by making measurements with pulses of shorter pulse width to check that the rise of the tail is indeed instantaneous.

5. Conclusion

We have investigated how optical pump–probe measurements may be used to study transient linear and circular birefringence at room temperature in semiconductors and both magnetic and non-magnetic metals. Measurements made on GaAs are consistent with optical orientation and relaxation of spin. However, the measured relaxation times depend on the pump fluence and suggest that interactions between excited carriers and renormalization of the band structure play an important role when the pump fluence is large. In the case of Ni, we could not detect any effect of the pump helicity on the picosecond demagnetization signal. This is unsurprising if excitation of an interband transition is essential for optical orientation of thermalized electron spins. While all three materials exhibit a peak in the transient rotation signal at zero delay, the dependence of the peak height on the helicity of the pump is markedly different in each case. The behaviour observed in GaAs is characteristic of circular birefringence (SIFE), that observed in Al is characteristic of linear birefringence (SOKE), while that in Ni has mixed character. Al also exhibits a longer-lived transient rotation signal that has the same dependence on the pump helicity as the zero-delay peak. This signal appears to rise instantaneously and relaxes with a time constant of 6 ps. We suggest that this transient is associated with an ultra-fast lattice distortion rather than optical orientation of spin. The development of a realistic microscopic model for the cubic optical non-linearity in Al is now required so that the origin of the transient rotation signal may be more clearly understood.

References

[1] See the articles by Vallée F and Bigot J-Y 2001 Trends in femtosecond lasers and technology *C. R. Acad. Sci., Paris* IV **2** 1469 and 1483
[2] Svirko Yu P and Zheludev N I 1998 *Polarization of Light in Nonlinear Optics* (New York: Wiley)

[3] Pierce D T and Meier F 1976 *Phys. Rev.* B **13** 5484
[4] Kikkawa J M and Awschalom D D 1998 *Phys. Rev. Lett.* **80** 4313
[5] Britton R S, Grevatt T, Malinowski A, Harley R T, Perozzo P, Cameron A R and Miller A 1998 *Appl. Phys. Lett.* **73** 2140
[6] Gupta J A, Knobel R, Samarth N and Awschalom D D 2001 *Science* **292** 2458
[7] Kimel A V, Bentivegna F, Gridnev V N, Pavlov V V, Pisarev R V and Rasing Th 2001 *Phys. Rev.* B **63** 235201
[8] Bungay A R, Popov S V, Shatwell I R and Zheludev N I 1997 *Phys. Lett.* A **234** 379
[9] Zheludev N I, Bennett P J, Loh H, Popov S V, Shatwell I R, Svirko Y P, Gusev V E, Kamalov V F and Slobodchikov E V 1995 *Opt. Lett.* **20** 1368
[10] Bennett P J, Albanis V, Svirko Y P and Zheludev N I 1999 *Opt. Lett.* **24** 1373
[11] Bennett P J, Malinowski A, Rainford B D, Shatwell I R, Svirko Yu P and Zheludev N I 1998 *Opt. Commun.* **147** 148
[12] Beaurepaire E, Merle J-C, Daunois A and Bigot J-Y 1996 *Phys. Rev. Lett.* **76** 4250
[13] Hohlfeld J, Matthias E, Knorren R and Bennemann K H 1997 *Phys. Rev. Lett.* **78** 4861
Hohlfeld J, Matthias E, Knorren R and Bennemann K H 1997 *Phys. Rev. Lett.* **79** 960
[14] Beaurepaire E, Maret M, Halté V, Merle J-C, Daunois A and Bigot J-Y 1998 *Phys. Rev.* B **58** 12134
[15] Conrad U, Güdde J, Jähnke V and Matthias E 1999 *Appl. Phys.* B **68** 511
[16] Zhang G P and Hübner W 2000 *Phys. Rev. Lett.* **85** 3025
[17] Zhang G P and Hübner W 1999 *J. Appl. Phys.* **85** 5657
[18] Güdde J, Conrad U, Jähnke V, Hohlfeld J and Matthias E 1999 *Phys. Rev.* B **59** R6608
[19] Koopmans B, van Kampen M, Kohlhepp J T and de Jonge W J M 2000 *J. Appl. Phys.* **87** 5070
[20] Koopmans B, van Kampen M, Kohlhepp J T and de Jonge W J M 2000 *Phys. Rev. Lett.* **85** 844
[21] Regensburger H, Vollmer R and Kirschner J 2000 *Phys. Rev.* B **61** 14716
[22] See discussion in the chapter by Zhang G, Hübner W, Beaurepaire E and Bigot J-Y 2002 *Spin Dynamics in Confined Magnetic Structures* vol 1, ed B Hillebrands and K Ounadjela (*Top. Appl. Phys.* **83** 245)
[23] Guidoni L, Beaurepaire E and Bigot J-Y 2002 *Phys. Rev. Lett.* **89** 17401
[24] Wilks R, Hughes N D and Hicken R J 2002 *J. Appl. Phys.* **91** 8670
[25] Ju G, Vertikov A, Nurmikko A V, Canady C, Xiao G, Farrow R F C and Cebollada A 1998 *Phys. Rev.* B **57** 700
[26] Elliot R J 1954 *Phys. Rev.* **96** 266
[27] Yafet Y 1963 *Solid State Physics* vol 14, ed F Seitz and D Turnbull (New York: Academic)
[28] Fabian J and Das Sarma S 1998 *Phys. Rev. Lett.* **81** 5624
[29] Fabian J and Das Sarma S 1999 *Phys. Rev. Lett.* **83** 1211
[30] Sambles J R, Cousins J E, Stesmans A and Witters J 1977 *Solid State Commun.* **24** 673
[31] Ashcroft N W and Mermin N D 1976 *Solid State Physics* (New York: Saunders)
[32] Jiles D C 1984 *Solid State Commun.* **51** 327
[33] Richardson C J K and Spicer J B 2002 *Appl. Phys. Lett.* **80** 2895
[34] Guo C, Rodriguez G, Lobad A and Taylor A J 2000 *Phys. Rev. Lett.* **84** 4493
[35] Kamprath T, Ulbrich R G, Leuenberger F, Münzenberg M, Sass B and Felsch W 2002 *Phys. Rev.* B **65** 104429-1
[36] Bauer M, Pawlik S and Aeschlimann M 1998 *Proc. SPIE* **3272** 201
[37] Richardson C J K 2000 *PhD Thesis* Johns Hopkins University